

Synthesis and electronic transport studies of CdO nanoneedles

Xiaolei Liu, Chao Li, Song Han, Jie Han^{a)} and Chongwu Zhou^{b)}

Dept. of E.E.-Electrophysics, University of Southern California, Los Angeles, California 90089

(Received 13 November 2002; accepted 21 January 2003)

Single-crystalline, needle-shaped CdO nanostructures were synthesized using a chemical vapor deposition method and characterized using a variety of techniques. Devices consisting of individual CdO nanoneedles were fabricated and high conductance as well as high carrier concentrations was observed. The temperature dependence of the conductance revealed thermal excitation as the dominating transport mechanism. Our devices exhibited good sensitivity to both infrared light and diluted NO₂ gas, indicating potential applications as infrared photodetectors and toxic gas sensors. © 2003 American Institute of Physics. [DOI: 10.1063/1.1562331]

In the past few years, extensive efforts have focused on the synthesis and characterization of one-dimensional (1-D) nanostructures, such as semiconductive nanowires,¹ largely driven by the need to understand properties of such structures and to develop their potential applications. Recent advances have led to integrated systems based on 1-D nanostructures^{2–4} and nanoscale chemical sensors with superior performance.^{5–7} Although nanowires made of conventional semiconductors have been thoroughly investigated, there is a lack of report on the synthesis and electronic transport properties of 1-D transparent conductive oxide (TCO) nanostructures, despite their enormous potential to be used in front panel displays and solar batteries.⁸ Among the TCO family, nanostructures based on CdO are particularly interesting because of their potential to serve as electrodes for nanoscale light-emitting diodes and lasers.⁹ In fact, bulk CdO shows a wide direct band gap of 2.27 eV and a narrow indirect band gap of 0.55 eV.¹⁰ Several techniques have been used to prepare polycrystalline CdO nanowires,¹¹ single crystalline nanobelts,¹² and microwhiskers,¹³ however, further investigations on the electrical, optical, and chemical properties of high-quality, 1-D, single-crystalline CdO nanostructures are still lacking. Here, we report the use of a chemical vapor deposition method to grow single-crystalline CdO nanoneedles and our investigations on their electronic, opto-electronic, and chemical sensing properties.

In our experiments, Si/SiO₂ substrates were cleaned and then coated with 20~30-Å gold, followed by baking the substrates under argon environment for half an hour, which served to break the gold thin film into separated gold catalytic nanoparticles. The cadmium source and the substrates were then loaded into the upper stream and the downstream of a quartz tube furnace, respectively. The substrates zone was heated up to 850~900 °C to activate the gold catalytic particles, followed by heating up the Cd source to 350 °C to generate Cd vapor, which was carried downstream by a constant argon flow with about 0.02% oxygen for about 30 min. After cooling down, the sample surfaces looked rough and showed a dark brown or crimson color. Figure 1 shows a

scanning electron microscope (SEM) image of the final product. The synthesized nanostructures appeared needle-shaped, with sharp tips about 40~100 nm in diameter and wide butts of several hundred nanometers to several micrometers at the other end, while the lengths of the nanoneedles normally ranged from 2 to ~20 μm. The inset of Fig. 1 shows a magnified view of the butt end of one nanoneedle, where a square cross section can be clearly seen. Our nanoneedles are distinctively different from the nanobelts obtained via direct evaporation and nucleation of CdO without any catalyst.¹² Instead, the formation of our CdO nanoneedles can be explained via the well-known vapor–liquid–solid (VLS) mechanism. Cd in the vapor phase first alloyed with the gold particles to form liquid droplets at high temperatures, and continued supply of Cd vapor pushed the Au/Cd solution beyond supersaturation. This led to nucleation of Cd, which immediately reacted with oxygen and resulted in the growth of CdO nanowires along the longitudinal direction. We suggest in addition to the conventional VLS growth process, the cadmium vapor and oxygen can also directly react and deposit on the CdO crystal surface, and therefore led to growth in the radial direction and larger diameters as time increased. This combined process thus yielded needle-shaped nanostructures with one end of smaller diameters determined by the size of the catalyst particles and the other end of larger diameters due to direct reaction and deposition on the sidewall.

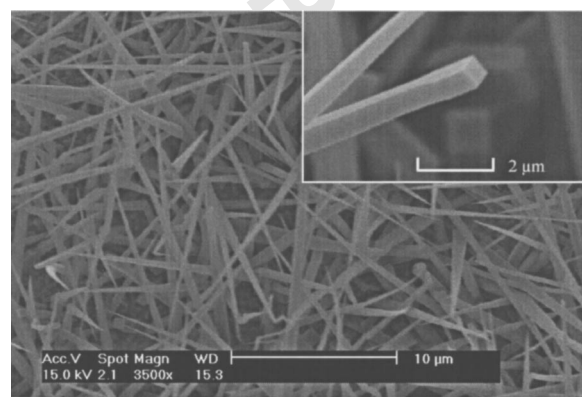


FIG. 1. SEM image of CdO nanoneedles grown using a chemical vapor deposition method. Inset: SEM image of a nanoneedle showing a square cross section.

^{a)}Elmet Corporation, NASA Ames Research Center, Moffett Field, CA 94035.

^{b)}Electronic mail: chongwuz@usc.edu

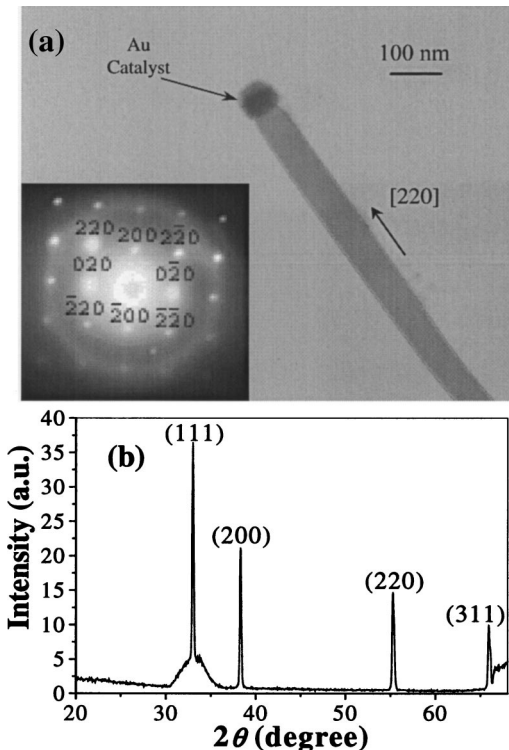


FIG. 2. (a) TEM image of a CdO nanoneedle with a catalyst particle at the very tip. Inset: SAED pattern of the CdO nanoneedle indicating the single-crystalline nature. (b) XRD pattern of CdO nanoneedles on a Si/SiO₂ substrate. Indices of the peaks are marked above the peaks.

Figure 2(a) shows a transmission electron microscope (TEM) image of the tip of a CdO nanoneedle. The Au/Cd alloy particle with a diameter around 60 nm can be clearly seen at the very tip, as expected from the VLS growth approach. The CdO nanoneedle appeared rather homogeneous and free of any domain boundaries, indicating the single-crystalline nature of our material. This was further confirmed by selective area electron diffraction (SAED) pattern recorded perpendicular to a nanoneedle long axis, as shown in the Fig. 2(a) inset. By analyzing the SAED pattern, we estimate the nanoneedles take a cubic crystal structure with a lattice constant of $4.70 \pm 0.18 \text{ \AA}$, close to 4.6953 \AA known for bulk CdO crystals.¹⁴ In addition, indexing the pattern identifies [220] direction as the VLS growth direction. We have performed SAED studies over many CdO nanoneedle samples and also at different locations along each nanoneedle, and similar diffraction pattern have been consistently observed. In addition, x-ray diffraction (XRD) analysis was also performed to confirm the crystal structure. Figure 2(b) shows a typical XRD pattern of our nanoneedle samples. Four peaks were observed in the XRD pattern and can be indexed to a rocksalt crystal structure of bulk CdO with a cell constant $a = 4.6953 \text{ \AA}$.¹⁴ No diffraction peaks corresponding to elemental Cd crystals were detected in any of our samples.

The synthesis and material analysis were followed by investigations of the electronic, optoelectronic, and chemical sensing properties of the CdO nanoneedles. The as-grown CdO nanoneedles were sonicated into a suspension in isopropanol and then dispersed onto a Si/SiO₂ substrate with pre-defined gold electrodes. Figure 3 inset shows a SEM image of a typical device, where a nanoneedle can be seen bridging

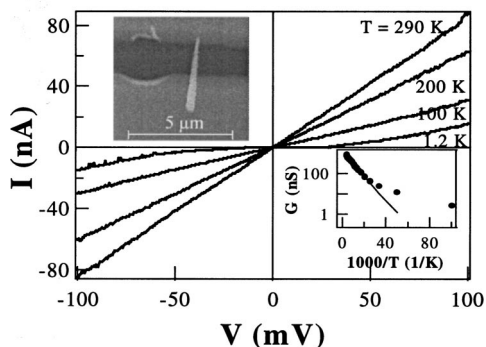


FIG. 3. Temperature-dependent I - V curves recorded with the temperature ranging from 290 K to 1.2 K. Upper-left inset: SEM image of a CdO nanoneedle between two Au/Ti electrodes. Lower-right inset: the nanoneedle conductance (in log scale) vs $1000/T$ (1/K).

two gold electrodes. Very often SEM inspection revealed nanoneedles shorter than those shown in Fig. 1, presumably because nanoneedles broke during the sonication process. Devices consisting of individual nanoneedles were chosen for detailed studies after a thorough SEM inspection, and very low two-terminal resistance $\sim 1 \text{ M}\Omega$ was consistently observed. This low resistance is in sharp contrast to the previous conclusion that the whiskers of CdO are highly resistive,¹³ therefore suggesting our CdO nanoneedles possess high quality and are free of current-blocking defects and domain boundaries. Figure 3 shows I - V curves of a typical CdO nanoneedle device at temperatures ranging from 290 to 1.2 K. At 290 K, the I - V curve appears very linear, indicating ohmic contacts were achieved between the metal electrodes and the nanoneedle. It is therefore reasonable to assume the two-terminal resistance is dominated by the nanoneedle instead of the contacts at room temperature. The shape of the nanoneedle segment between the electrodes resembles a truncated pyramid with the base 270 nm wide, the top 140 nm wide, and the edge 2 μm long, as determined by SEM inspection. The resistivity of the CdO nanoneedle is thus estimated to be $2.25 \times 10^{-4} \Omega \text{ cm}$ based on the device resistance ($1.14 \text{ M}\Omega$) and the nanoneedle geometry. This value is comparable with the resistivity measured on CdO films.^{15,16} We can further derive the carrier concentration to be around $1.29 \times 10^{20} \text{ cm}^{-3}$ by using a mobility value of $216 \text{ cm}^2 \text{ V}^{-1} \text{ s}^{-1}$ obtained from CdO films.¹⁶ Such a high carrier concentration is a result of oxygen vacancies and cadmium interstitials, which can serve as donor impurities.

An interesting feature shown in Fig. 3 is that the conductance monotonically decreased as the temperature decreased and the I - V curve developed a slight gap around zero bias voltage at 1.2 K. The conductance of the device in logarithm scale at zero bias voltage is plotted as a function of $1000/T$ in the lower-right inset of Fig. 3. For temperatures between 290 and 40 K, the conductance versus temperature can be fitted into the formula $G \sim \exp(-E_a/k_B T)$ with $E_a \sim 13.3 \text{ meV}$, suggesting thermal activation of carriers as the dominant transport mechanism. Below 40 K, the conductance was observed to deviate from the exponential fit. One possible explanation is related to the quantum mechanical tunneling, which dominates over the thermal emission at low temperatures. Similar transport mechanisms were observed before for nanotube devices.¹⁷ We did not find any evidence

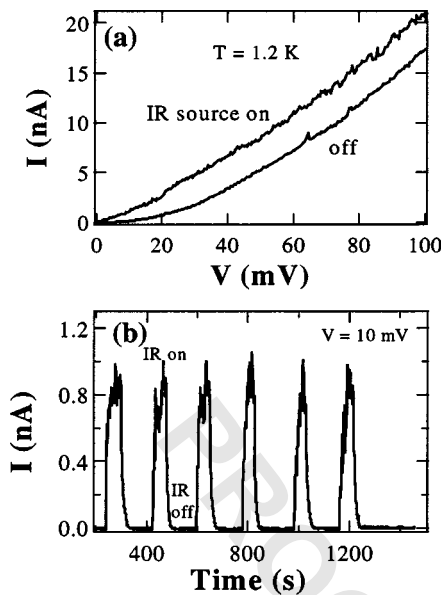


FIG. 4. (a) I - V curves measured at 1.2 K with the IR light source on and off, respectively. (b) Real-time measurement of IR response of the nanoneedle device. The IR source was turned on and off repeatedly with the device bias fixed at 10 mV.

of gate dependence from our devices, probably because our nanoneedles were degenerately n -type doped due to oxygen vacancies and cadmium interstitials and the gate-induced electric field can only affect the nanoneedles up to certain depth (~ 20 nm).

We notice that the large direct band gap of 2.28 eV which makes CdO a transparent conductive material was emphasized often in the literature,^{9,10,13} while the small indirect band gap of 0.55 eV received little attention. To clarify the role of this indirect band gap, we tested the response of our devices to IR light. The wavelength we chose for the test was 950 nm (1.3 eV), sufficient for absorption through the indirect band gap, but insufficient for the direct band gap. Experiments were carried out at 1.2 K to minimize the thermal excitation, and two I - V curves were taken with an IR light source (60 mW/cm 2) on and off respectively, as shown in Fig. 4(a). Pronounced response was observed, as manifested by the enhanced conduction under illumination. At zero bias, the conductance was 114.5 nS under illumination and 13.3 nS without illumination, indicating an on/off ratio of 8.6. Figure 4(b) shows the response of our CdO nanoneedle device to the IR illumination in real time. As the IR source was turned on and off, the nanoneedle device can be reversibly switched between high and low conductance states. The current increased instantly once the IR light source was turned on, but decayed relatively slowly when the light source was shut off. The current decay can be fitted into an exponential function as $I \propto e^{-(t-t_0)/\tau}$, where 8.6 s was found for τ . Our results clearly demonstrate that the indirect band gap of CdO has an important role and our nanoneedles could function as IR detectors.

As a semiconductive oxide, CdO devices are also expected to be sensitive to oxidative and reductive gases since the adsorption of such gas molecules on the surface leads to charge transfer and affects the carrier concentrations in CdO.¹⁸ Our motives of studying the chemical sensing properties of CdO nanoneedles lay on their relatively large

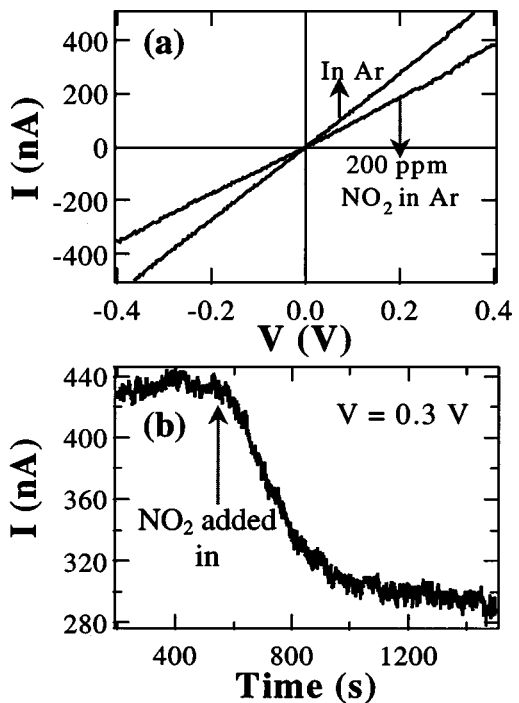


FIG. 5. (a) I - V curves measured at room temperature in Ar environment and in Ar mixed with 200-ppm NO₂, respectively. (b) Real-time response of the device upon exposure to 200-ppm NO₂ with the device bias fixed at 0.3 V.

surface-to-volume ratios compared to thin CdO films. We found that our CdO nanoneedles devices were sensitive to diluted NO₂ gas at room temperature. Figure 5(a) shows two I - V curves recorded before and after exposing the CdO nanoneedles device to 200 ppm NO₂ in Ar, where a suppression of the conductance from 1.37 to 0.91 μ S can be clearly seen. This indicates a reduction in the carrier concentration from 2.10×10^{20} cm $^{-3}$ before the exposure to 1.39×10^{20} cm $^{-3}$ after the exposure, with a reduction magnitude being 7.1×10^{19} cm $^{-3}$. Figure 5(b) shows the response of our device to 200-ppm NO₂ in real time. The conductance started to decrease immediately after the NO₂ exposure and saturated in about 400 s. We note that even though our devices are sensitive to NO₂, the on/off ratios and the response time are not as good as the values of gas sensors based on other nanowires.⁵⁻⁷ Nevertheless, considering our CdO nanoneedles have radial dimensions around hundreds of nanometers, the gas sensing properties can be substantially improved by using 1-D CdO structures with nanoscale diameters due to the enhanced surface-to-volume ratios.

In summary, single-crystalline CdO nanoneedles have been synthesized using a chemical vapor deposition technique. The crystal structure was verified to be cubic with a lattice constant ~ 4.7 Å using XRD and SAED techniques. Devices based on individual nanoneedles were fabricated and studied, which revealed carrier concentrations as high as 1.29×10^{20} cm $^{-3}$ and thermal activation with energy of 13.3 meV as the dominant transport mechanism. We have further demonstrated that CdO nanoneedle devices can absorb IR light via the indirect band gap with an on/off ratio of 8.6 at 1.2 K between the illuminated on state and the dark off state. Chemical sensing properties of CdO nanoneedle devices have also been studied, where 200-ppm NO₂ in Ar reduced

the carrier concentration by $7.1 \times 10^{19} \text{ cm}^{-3}$. Further optimization of the CdO nanostructures may lead to important applications as field emitters, nanoscale opto-electronic, and chemical sensing devices.

The authors thank Dr. J. Li and Dr. M. Meyyapan for valuable technical discussions. This work is supported by USC, a Powell award, NASA Contract No. NAS2-99092, NSF CAREER award, NSF NER program, and a Zumberger award.

¹C. M. Lieber, *Sci. Am.* **285**, 58 (2001).

²Y. Huang, X. Duan, Y. Cui, L. J. Lauhon, K.-H. Kim, and C. M. Lieber, *Science* **294**, 1313 (2001).

³X. Liu, C. Lee, J. Han, and C. Zhou, *Appl. Phys. Lett.* **79**, 3329 (2001).

⁴A. Bachtold, P. Hadley, T. Nakanishi, and C. Dekker, *Science* **294**, 1317 (2001).

⁵J. Kong, N. R. Franklin, C. Zhou, M. G. Chapline, S. Peng, K. Cho, and H. Dai, *Science* **287**, 622 (2000).

⁶Y. Cui, Q. Wei, H. Park, and C. M. Lieber, *Science* **293**, 1289 (2001).

⁷C. Li, D. Zhang, X. Liu, S. Han, T. Tang, J. Han, and C. Zhou (to be published).

⁸D. S. Ginley and C. Bright, *MRS Bull.* **25**, 58 (2000).

⁹T. J. Coutts, D. L. Young, and X. Li, *MRS Bull.* **25**, 15 (2000).

¹⁰H. Köhler, *Solid State Commun.* **11**, 1687 (1972); H. Finkenrath, *Z. An-gew. Phys.* **16**, 503 (1964).

¹¹Y. W. Wang, C. H. Liang, G. Z. Wang, T. Gao, S. X. Wang, J. C. Fan, and L. D. Zhang, *J. Mater. Sci. Lett.* **20**, 1687 (2001).

¹²Z. W. Pan, Z. R. Dai, and Z. L. Wang, *Science* **291**, 1947 (2001).

¹³N. Koparanova, Z. Zlatev, D. Genchev, and G. Popovich, *J. Mater. Sci.* **29**, 103 (1994).

¹⁴R. W. G. Wyckoff, *Crystal Structures* (Interscience, New York, 1968), Vol. 1, p. 86.

¹⁵Z. Zhao, D. L. Morel, and C. S. Ferekides, *Thin Solid Films* **413**, 203 (2002).

¹⁶X. Li, D. L. Young, H. Moutinho, Y. Yan, C. Narayanswam, T. A. Gessert, and T. J. Coutts, *Electrochem. Solid-State Lett.* **4**, C43 (2001).

¹⁷C. Zhou, J. Kong, and H. Dai, *Appl. Phys. Lett.* **76**, 1597 (2000).

¹⁸Y. Shimizu and M. Egashira, *MRS Bull.* **24**, 18 (1999).